ChemComm

COMMUNICATION

View Article Online
View Journal | View Issue

Cite this: *Chem. Commun.*, 2014, **50**, 4196

Received 8th January 2014,
Accepted 28th February 2014

DOI: 10.1039/c4cc00172a

www.rsc.org/chemcomm

A highly sensitive electrochemical genosensor based on Co-porphyrin-labelled DNA†

Iwona Grabowska,[a] Daniel G. Singleton,[b] Anna Stachyra,[c] Anna Góra-Sochacka,[c] Agnieszka Sirko,[c] Włodzimierz Zagórski-Ostoja,[c] Hanna Radecka,*[a] Eugen Stulz*[b] and Jerzy Radecki*[a]

We report the use of Co-porphyrins as electrochemical tags for a highly sensitive and selective genosensor. An avian influenza virus-based DNA sequence characteristic of H5N1 was detected at femtomolar levels from competing non-complementary sequences through hybridisation with the labeled DNA.

The development of a global community by improved travelling and globalisation brings along comfort in life that is unprecedented in history. Through the rapid movement of people and goods, together with a steady improvement in medical treatment, both the availability of products (in particular animals and food products) from far-away corners of the world as well as extended lifespans can be enjoyed. As a consequence, this brings about new challenges for society, particularly the fast and broad spread of local infectious diseases leading to an epidemic. The development of novel, very sensitive and fast analytical techniques for medical diagnostics, food control and environmental screening is therefore a high priority. Among a variety of available analytical techniques,[1] which are currently applied to these areas, the use of electrochemical genosensors is very promising as it can be applied using relatively simple instrumentation and shows a quick and sensitive response to the analyte.

Generally, in electrochemical genosensors the formation of the DNA duplex (hybridisation to an immobilised ssDNA) is monitored by changes in current or electrical potential values, either using label-free or labelled systems. Label-free genosensors can be based on the changes in oxidation/reduction peak current of electroactive oligodeoxynucleotides (ODNs) themselves,[2] on the use of ion-channels in amperometric sensors,[3] or include an electroactive intercalator;[4] the latter was shown to exhibit efficiencies in terms of electron transfer rates in the range of 1.5 to 40 s^{-1} and allows detecting sequence mismatches.[5] For the former systems, changes in response are a consequence of electrode surface changes after hybridisation inducing steric hindrance for marker ions to reach the surface of the electrode.[6] Redox labels are generally attached to the unbound end of the attached DNA (E-DNA), where ferrocene[7] (Fc) or methylene blue[8] are the most commonly used markers. In the "signal-off" architecture the electrochemical response is greatly diminished going from the flexible ssDNA to the rigid dsDNA,[9] whereas "signal-on" systems show the opposite effect.[10] The selectivity and sensitivity of the E-DNA sensors arises from a combination of a conformational change upon hybridisation, together with the redox labels being active at potentials far from those of the most electroactive biomolecules typical for clinical and environmental samples, thus being resistant to interfering contaminants. The E-DNA sensors reported to date can detect picomoles of ssDNA.[11]

We are now exploring the use of cobalt porphyrins as redox labels for genosensors based on gold electrodes (Scheme 1). The porphyrin is attached to the DNA close to the electrode surface, thus the distance does not vary greatly upon hybridisation. The generation of the analytical signal is proposed to proceed *via* a novel mechanism, which is not based on a signal-on or -off scheme. The sensitivity of this genosensor towards target DNA is in the femtomole range, offering orders of magnitude lower detection limits.

The synthesis of the porphyrin building block has been reported earlier;[12] the marker was introduced into ssDNA using standard phosphoramidite chemistry and automated SPS (see the ESI† for synthesis details). The porphyrin-DNA was metallated with cobalt post-synthetically. In order to anchor the DNA stably onto the gold surface, three dithiol and hexaethylene glycol units were added to the 5′-end, which ensures that the DNA is not released from the electrode at high voltages. The general layout and function of the genosensor is shown in Scheme 1. It consists of the porphyrin-DNA deposited onto the gold surface and embedded in a mercaptohexanol SAM (see the ESI† for details). The presence of the redox active probe (**CoP-ssDNA**) on the electrode surface was confirmed by cyclic voltammetry (CV)

[a] *Institute of Animal Reproduction and Food Research, Polish Academy of Sciences, Tuwima 10, 10-747 Olsztyn, Poland. E-mail: j.radecki@pan.olsztyn.pl; Fax: +48-895240124; Tel: +48-895234612*
[b] *School of Chemistry and Institute for Life Sciences, University of Southampton, Highfield, Southampton SO17 1BJ, UK. E-mail: est@soton.ac.uk; Tel: +44-2380599369*
[c] *Institute of Biochemistry and Biophysics, Polish Academy of Sciences, Pawińskiego 5A, 02-106 Warsaw, Poland*

† Electronic supplementary information (ESI) available: Synthesis of the porphyrin-DNA, preparation and characterisation of the Au-electrode. See DOI: 10.1039/c4cc00172a

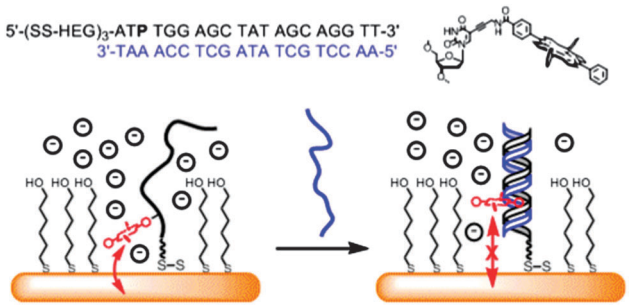

Scheme 1 Schematic illustration of the signal generation mechanism of the Co-porphyrin-DNA genosensor and sequences of the sensor and target strands (**P** denotes the site of porphyrin modification).

and differential pulse voltammetry (DPV). Representative cyclic CV spectra are shown in Fig. S1A in the ESI.† The quasi-reversible Co(II)/Co(III) redox processes[13] are visible at 0.285 ± 0.022 V and 0.190 ± 0.014 V for the electrode modified by **CoP-ssDNA.** DPVs show clearly visible oxidation and reduction peaks (Fig. S2, ESI†). The formation of the double helix at the surface of the electrode causes a small (a few mV) shift of oxidation and reduction peaks current towards a lower potential (Fig. S1B and S2B, ESI†). A similar phenomenon observed for ferrocene in mixed monolayers was reported by Creager *et al.*[14] The main Co(II)/Co(III) peak observed at ~0.3 V in CV (Fig. 1a) as well in DPV spectra (Fig. S2, ESI†) was used to determine the relationship between the concentration of target ssDNA and the electrochemical signal. A very small additional peak observed at ~0.45 V (ESI†) was not suitable; based on literature data,[13,15] we can assume that this small peak originated from catalytic activity of **CoP** leading to water oxidation and is also no longer visible after duplex formation. The density (Γ) of **CoP-ssDNA** assembled on the Au electrode surface was calculated based on the integration of the voltammetric peaks. The value of Γ obtained is equal to $1.1(\pm 0.3) \times 10^{-11}$ mol cm^{-2}, which represents 6.6×10^{12} molecules cm^{-2} and is in the same range as reported for other redox active DNA probes.[7b] CVs obtained for **CoP-ssDNA** at different scan rates from 10 to 10^3 mV s^{-1} (Fig. 1) show that the system becomes more irreversibly parallel with increasing scan rates. The linear relationship between the anodic and cathodic peak currents *vs.* the scan rate indicates that the redox process is not diffusion dependent and confirms the localisation of the **CoP-ssDNA** probe on the surface of the electrode. To find the relationship between the concentration of the target ssDNA sequence and the electrochemical signal, Osteryoung square-wave voltammetry (OSWV) was applied (Fig. 2), and representative OSWV spectra after incubation with the 20-mer complementary ssDNA are shown in Fig. 2a. Addition of the target ssDNA causes a decrease in the Co(III)/Co(II) Faradic current; the decrease is inversely proportional to the log of the concentration of the complementary ssDNA. A non-complementary ssDNA, on the other hand, induced much smaller changes in the current (Fig. 2b and c). The redox current *vs.* the log of the concentration of ssDNA follows a linear trend, from 10 to 80 fM (Fig. 2c). The genosensor displayed good selectivity. The slope of the calibration curve for complementary ssDNA was *ca.* 2.5 times higher in comparison to the slope recorded for non-complementary ssDNA. The estimated detection limit (DL = 2 × σ/S, where σ is the standard deviation of the response and S is the slope of the calibration curve)[15] is 21 fM. The precision, defined as the closeness of agreement among individual tests,[16] was very good (RSD = 3.6%; n = 5). Given that for the incubation we used 10 μl of the target DNA solution, the effective detection limit of DNA is 10^{-20} mol and amounts to 1000 DNA molecules; the electrode has a surface area of 2 mm^2 and contains about 1.3×10^{11} **CoP**-DNA molecules.

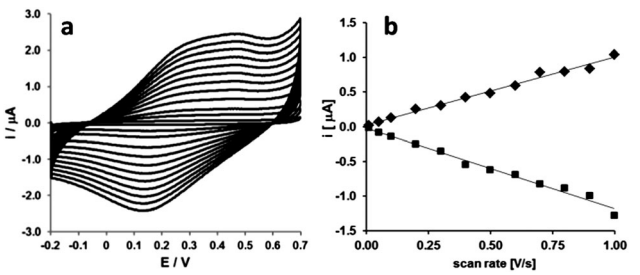

Fig. 1 (a) Cyclic voltammograms of **CoP-ssDNA** on the Au-electrode at scan rates from 10 to 1000 mV s^{-1}; buffer conditions: 1.0 M NaCl, 0.01 M sodium citrate, pH 7.0; (b) plots of anodic (◆) and cathodic (■) current *vs.* scan rate.

It should be noted that the sensitivity increased after storing the electrode in buffer solution at 4 °C for three days, which might be the result of restructuring and better ordering of the DNA on the electrode surface (Fig. S3, ESI†). The reusability of the genosensor was not tested as our future goal is the development a single-use miniaturized system.

The effect of ions on the electrochemical properties of monolayers with incorporated redox active sites has been reported mainly for ferrocene.[17] In order to determine the influence of different anions and cations on the value of the generated signal, we evaluated the relationship between the scan rate and anodic and cathodic peak potentials measured for **CoP-ssDNA** and **CoP-dsDNA**, in the presence of different supporting electrolytes (CsCl, KCl, NaCl, $NaNO_3$, $NaBF_4$ and $NaClO_4$) at 1.0 M concentration buffered with 0.01 M sodium citrate (Fig. S4, ESI†). For electrolytes containing Cl^-, CV spectra recorded for K^+ and Na^+ were very similar with a clearly visible reduction process. In the presence of the most lipophilic cation, Cs^+, the Co(II)/Co(III) Faradaic current was almost invisible. When different anions (such as Na^+ salts) were investigated, the reduction processes were better visible in the presence of more lipophilic anions such as NO_3^- and BF_4^- (Fig. S4, ESI†). The shift of oxidation and reduction potentials to higher values follows the increase of lipophilicity and size of both cations and anions, and was observed for both ssDNA and dsDNA (Table S1, ESI†). The values of the electron transfer coefficient (α) and electron rate constant (k) measured using different electrolytes are collected in Table S2, ESI.† In most cases, the α values are >0.5, indicating that the reduction is favoured,[18] and only the most lipophilic Cs^+ cation has α values <0.5, and thus favours oxidation. For BF_4^- the α values are close to 0.5 indicating energy symmetry for the redox reactions. k values are higher for chlorides, compared to the values measured in the presence of more lipophilic anions. For all electrolytes studied, reduction is superior to oxidation. Based on these observations, NaCl is the most suitable supporting electrolyte as it is the least lipophilic salt for use with **CoP-ssDNA** and **CoP-dsDNA**. Overall, the influence of different anions and cations on the redox properties of

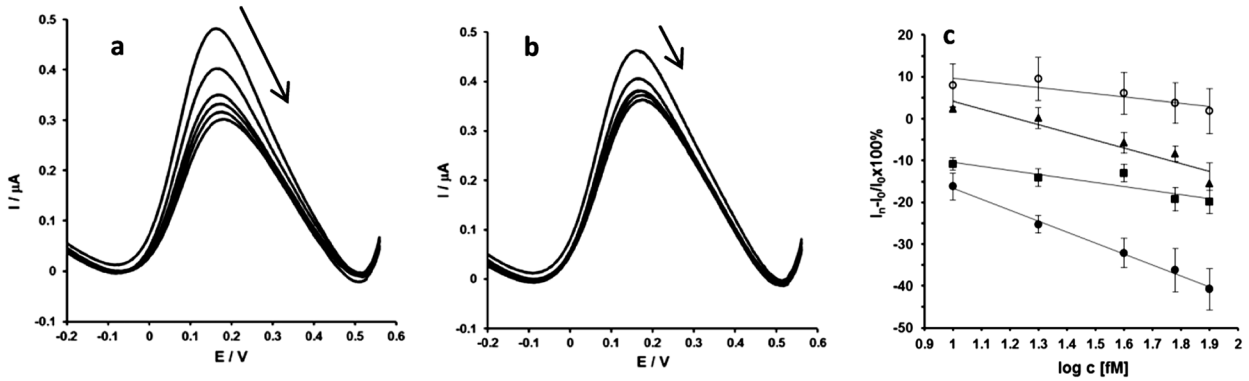

Fig. 2 Representative Osteryoung square-wave voltammograms (OSWVs; 1 mV, square-wave frequency: 50 Hz and amplitude: 25 mV) obtained for the electrode modified by Co-porphyrin-ssDNA probe: 5′-A**P**T TGG AGC TAT AGC AGG TT-3′ (a) after hybridisation with 20-mer complementary ssDNA and (b) in the presence of the sequence with three complementary bases at concentrations of 0, 10, 20, 40, 60 and 80 fM (buffer conditions: 0.09 M NaCl, 0.09 M sodium citrate, pH 7.0). (c) Relative intensity of redox Co(II)/Co(III) current *vs.* log of the concentration of 20-mer complementary ssDNA 5′-**AAC CTG CTA TAG CTC CAA AT**-3′; (●) sequence with three complementary bases: 5′-GGA G**T**T **C**CT CTC TCA TC**A** TC-3′; (■), sequence with one complementary base.: 5′-G**A**A GAA GAG AGA GGA ACT CC-3′; (▲) fully non-complementary sequence.: 5′-TTG GAC GAT ATC GAG GTT TA-3′.

cobalt porphyrins is not only governed by their lipophilicity or size, but the affinity towards the cobalt site is likely to be a second parameter in the process. However, the access of the most hydrophilic Cl^- and Na^+ ions to the Co(II) redox sites seems difficult. Therefore, the oxidation and reduction processes are hindered, due to which a large decrease of the Co(II)/Co(III) redox current upon hybridisation with complementary DNA is observed.

The majority of the recently developed electrochemical DNA or PNA sensors make use of the hybridisation process which alters the distance of the redox label[8,9] (*e.g.* Fc) from the electrode surface. In our system, the redox centre is located close to the electrode surface, thus the change in distance is relatively small. In this respect our sensor does not directly rely on the "signal on/off" mechanism through changes in distance but rather through changes in the hydrophobic environment of the label. The influence of the parameters on redox reactions in electroactive SAMs has been studied extensively.[19] In particular, the solvent effect (stabilisation of a specific state of the redox couple) and the double layer effect (prevention of counter-ions from solution entering the SAMs) are described by the Smith and White[20] model as well as by Creager.[14] In consequence, either the Gibbs free energy (ΔG^o) of solvation or the spatial distribution of ions in the interfacial region is changed. For our system the hybridisation process leads to two changes in the electrode surface environment: (i) the **CoP** redox centre is more embedded in the ODN duplex, and (ii) a duplication of the negative charge makes the molecular environment around the porphyrin more polar. Both factors have an influence on the redox reaction by creating a hindrance for the anionic counterions to be transported to the redox centre, leading to a decrease in the Faradic current. This is in line with reports on using an Fc label to detect biotin–IgG antibody interactions, where the antibody sensing caused a modulation of the Fc electrochemistry due to the restricted access of counter ions to the redox probe.[21]

In summary, we have presented a new type of electrochemical genosensor based on gold electrodes modified by a cobalt porphyrin DNA probe, where the probe is located very close to the surface of the electrode. The genosensor displays very good selectivity and sensitivity at the femtomolar concentration level towards 20-mer ssDNA derived from avian influenza virus type H5N1. SWV was applied as a sensing technique, and the changes in the Co(II)/Co(III) Faradic current were used as an analytical signal. The signal changes are a consequence of both solvent and double layer effects, and are strongly dependent on the supporting electrolyte. The high sensitivity, low detection limit, selectivity towards complementary DNA and the ease of microelectrode formation show high potential of the sensor system for applications in medical diagnostics.

This work was supported by the Innovative Economy Program, Grant No. WND-POIG.01.01.02-00-007/08. Mass spectrometry data were acquired at the EPSRC UK National Mass Spectrometry Facility at Swansea University. Support by the BBSRC (DTA to DGS) is also greatly acknowledged.

Notes and references

1 (*a*) S. Duraipandian, M. S. Bergholt, W. Zheng, K. Y. Ho, M. Teh, K. G. Yeoh, J. B. Y. So, A. Shabbir and Z. W. Huang, *J. Biomed. Opt.*, 2012, **17**, 081418; (*b*) H. Hahn, J. D. Pallua, C. Pezzei, V. Huck-Pezzei, G. K. Bonn and C. W. Huck, *Curr. Med. Chem.*, 2010, **17**, 2956–2966.
2 (*a*) E. Palecek, *Electroanalysis*, 2009, **21**, 239–251; (*b*) E. Palecek and M. Bartosik, *Chem. Rev.*, 2012, **112**, 3427–3481.
3 (*a*) H. Aoki and Y. Umezawa, *Electroanalysis*, 2002, **14**, 1405–1410; (*b*) Y. Umezawa and H. Aoki, *Anal. Chem.*, 2004, **76**, 320A–326A.
4 (*a*) E. M. Boon, N. M. Jackson, M. D. Wightman, S. O. Kelley, M. G. Hill and J. K. Barton, *J. Phys. Chem. B*, 2003, **107**, 11805–11812; (*b*) E. E. Ferapontova, *Curr. Anal. Chem.*, 2011, **7**, 51–62.
5 (*a*) A. Abi and E. E. Ferapontova, *J. Am. Chem. Soc.*, 2012, **134**, 14499–14507; (*b*) A. Anne, A. Bouchardon and J. Moiroux, *J. Am. Chem. Soc.*, 2003, **125**, 1112–1113.
6 (*a*) K. Malecka, I. Grabowska, J. Radecki, A. Stachyra, A. Gora-Sochacka, A. Sirko and H. Radecka, *Electroanalysis*, 2012, **24**, 439–446; (*b*) K. Malecka, I. Grabowska, J. Radecki, A. Stachyra, A. Góra-Sochacka, A. Sirko and H. Radecka, *Electroanalysis*, 2013, **25**, 1871–1878.
7 (*a*) J. Zhao, X. L. He, B. Bo, X. J. Liu, Y. M. Yin and G. X. Li, *Biosens. Bioelectron.*, 2012, **34**, 249–252; (*b*) J. Y. Zhuang, L. B. Fu, D. P. Tang, M. D. Xu, G. N. Chen and H. H. Yang, *Biosens. Bioelectron.*, 2013, **39**, 315–319.
8 (*a*) E. Farjami, R. Campos and E. E. Ferapontova, *Langmuir*, 2012, **28**, 16218–16226; (*b*) E. Farjami, L. Clima, K. Gothelf and E. E. Ferapontova, *Anal. Chem.*, 2011, **83**, 1594–1602.
9 (*a*) I. Grabowska, K. Malecka, A. Stachyra, A. Gora-Sochacka, A. Sirko, W. Zagorski-Ostoja, H. Radecka and J. Radecki, *Anal. Chem.*, 2013, **85**,

10167–10173; (*b*) F. Ricci, G. Adornetto, D. Moscone, K. W. Plaxco and G. Palleschi, *Chem. Commun.*, 2010, **46**, 1742–1744.
10 C. E. Immoos, S. J. Lee and M. W. Grinstaff, *J. Am. Chem. Soc.*, 2004, **126**, 10814–10815.
11 S. Butow and F. Lisdat, *Electroanalysis*, 2010, **22**, 931–937.
12 (*a*) A. Brewer, G. Siligardi, C. Neylon and E. Stulz, *Org. Biomol. Chem.*, 2011, **9**, 777–782; (*b*) L. A. Fendt, I. Bouamaied, S. Thöni, N. Amiot and E. Stulz, *J. Am. Chem. Soc.*, 2007, **129**, 15319–15329.
13 (*a*) X. Q. Lu, L. M. Zhang, M. R. Li, X. Q. Wang, Y. Zhang, X. H. Liu and G. F. Zuo, *ChemPhysChem*, 2006, **7**, 854–862; (*b*) Q. Wang, F. P. Zhi, W. T. Wang, X. H. Xia, X. H. Liu, F. F. Meng, Y. Y. Song, C. Yang and X. Q. Lu, *J. Phys. Chem. C*, 2009, **113**, 9359–9367.
14 S. E. Creager and G. K. Rowe, *J. Electroanal. Chem.*, 1997, **420**, 291–299.
15 D. Wang and J. T. Groves, *Proc. Natl. Acad. Sci. U. S. A.*, 2013, **110**, 15579–15584.
16 M. E. Swartz and I. S. Krull, *Handbook of Analytical Validation*, CRC Press, Taylor and Francis Group, London, 2012.
17 (*a*) A. V. Rudnev, U. Zhumaev, T. Utsunomiya, C. J. Fan, Y. Yokota, K. Fukui and T. Wandlowski, *Electrochim. Acta*, 2013, **107**, 33–44; (*b*) G. Valincius, G. Niaura, B. Kazakeviciene, Z. Talaikyte, M. Kazemekaite, E. Butkus and V. Razumas, *Langmuir*, 2004, **20**, 6631–6638.
18 A. J. Bard and L. R. Faulkner, *Electrochemical Methods-Fundamentals and Applications*, John Wiley & Sons Inc., New York, 2nd edn, 2001.
19 G. K. Rowe and S. E. Creager, *Langmuir*, 1991, **7**, 2307–2312.
20 C. P. Smith and H. S. White, *Anal. Chem.*, 1992, **64**, 2398–2405.
21 (*a*) J. J. Gooding, A. Chou, F. J. Mearns, E. Wong and K. L. Jericho, *Chem. Commun.*, 2003, 1938–1939; (*b*) S. M. Khor, G. Z. Liu, C. Fairman, S. G. Iyengar and J. J. Gooding, *Biosens. Bioelectron.*, 2011, **26**, 2038–2044.